ELSEVIER

European Journal of Pharmaceutics and Biopharmaceutics 48 (1999) 1–12

European Journal of Pharmaceutics and Biopharmaceutics

Research paper

Evaluation of aminoalkylmethacrylate nanoparticles as colloidal drug carrier systems. Part II: characterization of antisense oligonucleotides loaded copolymer nanoparticles

H.-P. Zobel[a], F. Stieneker[c], S. Atmaca-Abdel Aziz[b], M. Gilbert[b], D. Werner[b], C. R. Noe[b], J. Kreuter[a], A. Zimmer[a,*]

[a]*Institut für Pharmazeutische Technologie, Johann Wolfgang Goethe-Universität, Frankfurt am Main, Germany*
[b]*Institut für Pharmazeutische Chemie, Johann Wolfgang Goethe-Universität, Frankfurt am Main, Germany*
[c]*Arbeitsgemeinschaft für Pharmazeutische Verfahrenstechnik, Mainz, Germany*

Received 7 April 1998; accepted 4 January 1999

Abstract

Aminoalkylmethacrylate methylmethacrylate copolymer nanoparticles were evaluated for their use as potential drug carrier systems. Their cytotoxicity, as well as the loading of antisense oligonucleotides that were employed as anionic model drugs depended on the substitution of the basic aminoalkyl copolymer. Toxic influences on the integrity of cell membranes depended on aminoalkyl groups located on the particle surfaces. Toxicity was observed either by 3-[4,5-dimethylthiazol-2-yl]-2,5-diphenyltetrazolium bromide (MTT) assays using African green monkey kidney (AGMK) cells or by a hemolysis test, where the efflux of haemoglobin from disrupted erythrocytes was measured. The cytotoxic effects were increased by the elongation of the *N*-alkyl chain by four additional methylene groups. Lipophilic polymethylmethacrylate (PMMA) homopolymer nanoparticles showed a negative surface charge and, therefore, were not suitable for the adsorption of anionic drugs. The surface charge was changed to positive values by the incorporation of basic monomers. Consequently, the loading efficacy was increased by raising the basic copolymer portion. Additionally, a pH-dependent loading behaviour of oligonucleotides was observed. Substitution of the amino nitrogen protons by methyl groups led to a decreased oligonucleotide loading and to a reduced cytotoxicity. Nanoparticles with permanent positively charged quarternary ammonium groups showed a high pH-independent loading efficacy, but also possessed a high cytotoxic potential. In this study, cationic copolymer nanoparticles containing 30% (w/w) methylaminoethyl-methacrylate (MMAEMC) were found to be optimal with regard to biocompatibility and carrier properties for hydrophilic anionic antisense oligonucleotides. A significant portion of adsorbed oligonucleotides were protected from enzymatic degradation. The cellular uptake of oligonucleotides into Vero cells was significantly enhanced by this methylaminoethyl-methacrylate derivative.

Keywords: Nanoparticles; Aminoalkylmethacrylate; Methylmethacrylate; Surface charge; Antisense oligonucleotides; Loading efficacy; 3-[4,5-Dimethylthiazol-2-yl]-2,5-diphenyltetrazolium bromide; Hemolysis; Cell-uptake

1. Introduction

Acrylic acid derivatives such as poly(alkylcyanoacrylates) and poly(alkylmethacrylates) are the most frequently used polymers for the preparation of nanoparticles [1–4]. However, these compounds are not suitable for the adsorption of hydrophilic ionic drugs due to their hydrophobicity. In Part I of this study, monomers based on differently sub-

* Corresponding author. Institut für Pharmazeutische Technologie, Johann Wolfgang Goethe-Universität, Biozentrum, Marie-Curie-Straße 9, 60439 Frankfurt am Main, Germany. Tel.: +49-69-798-29692; fax: +49-69-798-29694; e-mail: zimmer@em.uni-frankfurt.de

0939-6411/99/$ - see front matter
PII: S0939-6411(99)00003-X

stituted aminoalkylmethacrylate derivatives were developed and optimized [5]. Copolymerization with methylmethacrylate resulted in stable nanoparticle suspensions with a strong positive surface charge. Particle diameters and zeta potentials of these nanoparticles at different pH values were shown to be dependent on the molecular structure of the basic aminoalkylmethacrylate comonomer, the monomer ratio, and the polymerization conditions.

The objective of the present study was to assess the biocompatibiliy of these copolymer nanoparticles for an application in cell cultures and in vivo. Furthermore, the loading capacity of these carriers for antisense oligonucleotides as anionic hydrophilic model drugs were investigated. Antisense oligodeoxynucleotides are short segments of single stranded DNA or DNA derivatives. They act as highly sequence-specific modulators of genetic expression [6] and, therefore, may be used for the treatment of viral diseases [7,8], cancer [9], or other diseases based on an uncontrolled overexpression of proteins. The base sequences of oligonucleotides are complementary to the mRNA transcripts of the targeted genes. Hybridization to the coding (sense) sequences in the mRNA targets by Watson–Crick base pairing inhibits the translation or processing of the viral mRNA. In the past, most frequently phosphorothioate derivatives were used in antisense therapy due to an enhanced enzymatic stability. These drugs are also polyanionic macromolecules and, therefore, they do not sufficiently permeate lipid bilayers. In this context, we have investigated nanoparticles as cell penetration enhancers initially in one of our earlier studies [10]. Also, other work groups evaluated nanoparticles as drug delivery systems for oligonucleotides [11–14]. These previous studies showed that oligonucleotides were bound to alkylcyanoacrylate nanoparticles either by incorporated diethylaminoethyl (DEAE) dextran or in combination with the lipophilic ion-pair compound cetyltrimethylammonium bromide (CTAB). In contrast to these previously published concepts, the aim of the present paper was the development of positively charged copolymer nanoparticles without further ionic ingredients which might reduce the biocompatibility. Finally, the most biocompatible nanoparticles were investigated in terms of cellular uptake enhancement for antisense oligonucleotides.

2. Materials and methods

2.1. Materials

The monomer *N*-trimethylaminoethylmethacrylate chloride (TMAEMC) and ammonium persulfate (APS) were a gift provided by A.G. Hüls (Marl, Germany), the monomer *N*-dimethylaminoethylmethacrylate (DMAEMC) was purchased from Fluka (Buchs, Switzerland). The basic monomers aminoethylmethacrylate (AEMC), *N*-monomethylaminoethylmethacrylate (MMAEMC), aminohexylmethacrylamide (AHMAC), and *N*-trifluoroacetyl protected aminohexylmethacrylate (AHMC) are not commercially available and, therefore, were synthesized as described in Part I of this publication [5]. Methylmethacrylate (MMA) as well as all other chemical compounds used for the preparation of nanoparticles and the subsequent loading studies were purchased from Merck (Darmstadt, Germany). 3-[4,5-Dimethylthiazol-2-yl]-2,5-diphenyltetrazolium bromide (MTT) and Triton 100 were obtained from Sigma (Deisenhofen, Germany). Earle's minimal essential medium (MEM), fetal bovine serum (FBS) as well as all other cell-culture supplements were provided by Seromed (Biochrom KG, Berlin, Germany). The unmodified antisense oligonucleotides and 5′-fluorescein labelled oligos were synthesized by MWG Biotech (Ebersberg, Germany). All oligonucleotides were purified by HPLC and were checked for full-length by SAX-HPLC. The other chemicals were of analytical grade and were used as obtained.

2.2. Preparation of nanoparticles

The different methacrylate copolymer nanoparticles consisting of 70% (w/w) MMA and 30% (w/w) of one of the basic monomers were produced by free radical polymerization as previously described [5,15]. Briefly, methylmethacrylate and the basic aminoalkylmethacrylate monomer were dissolved in preheated water or in water acetone mixtures at 78°C. At this temperature, ammonium persulfate was added as polymerization initiator (0.03% w/w). During the preparation, the reaction mixture was stirred on a thermostated well plate (H + P Labortechnik GmbH, München) in tightly closed beakers of 100 ml at 400 rpm. After 24 h, when polymerization was completed, the acetone of the polymerization medium was evaporated for 1 h. The formed nanoparticles were concentrated to a polymer content between 5 and 20% (w/v) with an ultrafiltration unit (model 402, Amicon, Witten, Germany) equipped with a Diaflo YC05 filtration membrane (Amicon) in order to obtain stock suspensions. The toxicity and loading studies were performed using stock suspensions purified by dialysis through a semipermeable membrane with an exclusion size of 12 000–14 000 dalton (Dialysis Tubing-Visking, Medicell, London, UK). Nanoparticles prepared with TMAEMC were lyophilized after purification (Lyovac GT2, Leybold Heraeus, Hürth, Germany). Resuspension of dried nanoparticles was performed using ultrasonication (Transsonic Digital, Elma, Singen, Germany). The copolymerization of aminohexylmethacrylate with methylmethacrylate was performed by using the *N*-trifluoroacetyl protected compound because of the instability of the pure basic monomer. The aminohexyl groups on the surface of these particles were deprotected in a 12.5% ammoniumhydroxide solution by autoclaving at 2 bar and 121°C for 1 h. Subsequently, the deprotected aminohexylmethacrylate-methylmethacrylate copolymer nanoparticles were immediately purified by dialysis.

2.3. Size determination of nanoparticles

The particle diameters were measured by photon correlation spectroscopy (PCS). The PCS instrument consisted of a BI-200 SM Goniometer Ver. 2.0 (Brookhaven Instruments, Holtsville, NY), equipped with a 30 mW He-Ne-Laser (Melles Griot, Cincinnati, CA), and was connected to a BI-2030 AT Digital Correlator (Brookhaven Instruments, Holtsville, NY). The measurements were carried out at a scattering angle of 90° and a temperature of 25°C. The count rate was adjusted to 20–30 kHz by diluting each sample with deionized, filtered water (0.22 mm cellulose nitrate filter, Schleicher&Schuell, Dassel, Germany) or phosphate buffer solutions, respectively.

2.4. Surface charge

The surface charge (zeta potential) was determined by measuring the electrophoretic mobility of the nanoparticles using a Lazer Zee Meter Model 501 (PenKem, Bedford Hills, NY). Samples were adjusted to a final concentration of 100 mg/ml by diluting the dialyzed stock suspensions with deionized water or different phosphate buffers. The measured zeta potential was calculated and corrected for a standard reference temperature of 20°C.

2.5. Cytotoxicity studies

2.5.1. MTT assay

African green monkey kidney cells (AGMK) were seeded into 96-well-plates at a density of 3×10^4 cells/well using Earle's minimal essential medium (MEM) supplemented with 7% (v/v) FBS. The cells were washed using phosphate buffered saline (PBS) pH 7.4 and incubated with 100 ml nanoparticle suspension diluted to the desired final concentration using MEM cell culture medium. One hundred microlitres MEM medium and 50 ml MTT solution prepared of 3-[4,5-dimethylthiazol-2-yl]-2,5-diphenyltetrazolium bromide (2.5 mg/ml PBS) were added after 4 and 24 h, respectively. The cells were kept at 37°C and 5% (v/v) CO_2 in a cell culture incubator model BB6220 (Haereus, Germany). Two hours later the supernatants were removed after centrifugation at 400 × g for 5 min (plate rotor 16M2/MT connected to the centrifuge 5403, Eppendorf, Hamburg, Germany) and the cells were lysed by the treatment with a solution of 25% sodium dodecylsulfate (SDS) in 0.1 M NaOH for 24 h at 37°C. The quantification of the resulting blue dye was performed by a multiwell scanning spectrophotometer (MR 5000, Dynatech, Denkendorf, Germany) at a wavelength of 550 nm and a reference wavelength of 630 nm.

2.5.2. Hemolysis assay

Human erythrocytes were prepared from a blood conserve as described previously [16]. Erythrocytes were separated from 30 ml blood by centrifugation at 1000 × g (GPR centrifuge, Beckmann, Munich, Germany) for 20 min. Ten millilitres of pellet was washed three times with 30 ml phosphate buffered saline (PBS, 154 mM sodium chloride, 10 mM phosphate, pH 7.4) to remove residual blood plasma. Two millilitres of the purified erythrocytes were resuspended with 38 ml PBS to adjust a final hematocrit of 5%. Fifty micro litres of the resulting suspension was incubated with 1000 ml of the different nanoparticle preparations in PBS at 37°C and 700 rpm (Thermomixer 5436, Eppendorf, Hamburg, Germany) for 30 min. Various particle concentrations were chosen ranging from 10 to 1000 mg/ml. The content of haemoglobin released from disrupted erythrocytes was determined photometrically at 576 nm (U 3000, Hitachi, Tokyo, Japan) in the supernatant after centrifugation at 1000 × g for 5 min (centrifuge 5417, Eppendorf, Hamburg, Germany). The percentage of hemolysis was calculated on the basis of the 100% hemolysis induced by the supplement of a 1% (w/w) solution of Triton 100 in PBS pH 7.4. The 0% control was obtained by addition of pure PBS. The calibration of the assay was performed by the dilution of the totally lysed erythrocyte sample with different amounts of PBS pH 7.4.

2.6. Determination of the oligonucleotide content

The determination of the oligonucleotide concentrations in loading experiments was performed by a strong anion-exchange HPLC assay, using a Dionex Nucleopac PA 100 4 × 250 column (Dionex, Idstein, Germany) and a Merck-Hitachi HPLC-system (Merck, Darmstadt, Germany). The HPLC system was equipped with an autosampler AS-2000A, a L-6220 gradient pump, an interface D-6000A, a diode-array-detector (DAD) L-4500, and the DAD system manager model D-6500. The gradient pump used a two-eluent system. Eluent A was prepared by dissolving 50 mM sodium chloride in 25 mM sodium hydroxide solution, eluent B contained 1 M NaCl in 25 mM NaOH. A linear eluent gradient from 145 to 1000 mM sodium chloride and a flow rate of 1 ml/min was used for 20 min. Initial gradient conditions were reconstituted after 36 min. From each sample 20 ml were injected. The oligonucleotide concentration was determined by measuring the absorbance at 260 nm.

2.7. Oligonucleotide loading

The oligonucleotide used in this study consisted of 19 nucleotides (sequence 5′-ACG TTC CTC CTG CGG GAA G-3′, MW 5799.8) and possessed an unmodified phosphodiester backbone. Oligonucleotide loading to the nanoparticle polymer was achieved by adsorption. The influence of the basic copolymer content and different media on the loading characteristics of the copolymer nanoparticles were investigated in this study.

The influence of the basic copolymer content was investigated at a fixed oligonucleotide concentration (15 mg/ml)

and nanoparticle concentration (100 mg/ml) using 10 mM phosphate buffer pH 5.5.

Solutions with various oligonucleotide concentrations (2–60 mg/ml) were incubated with 100 mg/ml of nanoparticles in the presence of different loading media. Deionized water and various phosphate buffer solutions (pH 5.5 10 mM; pH 5.5, 150 mM; pH 7.4, 10 mM; pH 7.4, 150 mM) were employed.

The nanoparticles were incubated with oligonucleotides for about 12 h at 20°C in deionized water or the phosphate buffer solutions. Finally, the non-adsorbed oligonucleotides were separated from the particles by ultracentrifugation at 100 000 × g (Ultracentrifuge Optima L-80, Beckmann, Germany). Quantification of the oligonucleotides in the supernatant was performed by the HPLC assay as described above. The oligonucleotide portion bound to nanoparticles was taken as the difference between the amount of oligonucleotide added for incubation and the measured oligonucleotide concentration in the supernatant.

2.8. Oligonucleotide protection

The protective effect of the oligonucleotide nanoparticle complex against DNase I digestion was investigated for MMAEMC nanoparticles used for the cell-uptake assay. Oligonucleotides (10 mg/ml) were adsorbed to 100 mg/ml MMAEMC nanoparticles in 10 mM phosphate buffer (pH 5.5). The nanoparticle preparation as well as the unprotected oligonucleotide control were incubated with 10 IU/ml DNase I at 37°C and 700 rpm using an Eppendorf thermomixer 5436 (Eppendorf, Germany) for 30 min. Twenty microlitres of a DNase I solution (30 mg/ml in 25 mM Tris-(hydroxymethyl)-aminomethane, 5 mM magnesium chloride, 0.1 mM EDTA, pH 7.4) were added to 100 ml of each sample. After digestion, enzyme-inactivation was achieved by the addition of 25 ml 1 M EGTA solution and the ODN nanoparticle complex was dissociated by a further treatment with 50 ml 0.1 M sodium hydroxide solution for 1 h. Oligonucleotides and their digested fragments were determined by HPLC as described above.

2.9. Cell-uptake study

2.9.1. TRITC-labelling of MMAEMC nanoparticles

One millilitre of a MMAEMC nanoparticle suspension (60 mg/ml) was adjusted to pH 9.0 using sodium hydroxide solution. The suspension was permanently stirred at 0°C. 120 ml of an ice-cooled solution of the tetramethylrhodamine isothiocyanate (TRITC) dye Texas Red (sulforhodamine 101 acid chloride, 1 mg ml^{-1}) was carefully added and, further on, the reaction mixture was kept stirring at the same temperature for another 4 h. These conditions and ratio between nanoparticles and tetramethylrhodamine isothiocyanate led to a quantitative binding of the dye and was determined photometrically after centrifugation.

2.9.2. Culture of Vero cells

Vero (African green monkey kidney) cells were grown in Earle's minimal essential medium supplemented with 3.5% (v/v) new-born bovine serum, 3.5% (v/v) fetal bovine serum, penicilline, streptomycin, non essential amino acids, and l-glutamine in a humidified incubator containing 5% CO_2 at 37°C.

FODN/nanoparticle formulations, unbound FITC oligonucleotides, as well as TRITC-labelled MMAEMC nanoparticles were diluted 10-fold with MEM cell culture medium to an oligonucleotide concentration of 10 mg/ml and a final particle concentration of 100 mg/ml. An aliquot was taken to determine enzymatic degradation and was processed as described above after 4 h incubation. A confluent layer of approximately 3×10^4 Vero cells was incubated with these preparations in 16-well tissue culture chamber slides (Lab-Tek, Nunc, Naperville, IL) at 4 and at 37°C, respectively. After 4 h of incubation the cells were washed three times with cold PBS pH 7.4 to remove residual FODN-preparations and cell culture medium. Cell membranes were stained by incubation with TRITC-concanavalin A or FITC-concanavalin A (50 mg/ml PBS) for 1 min. The cells were rinsed three times with cold PBS pH 7.4 and fixed with a 5% (w/w) paraformaldehyde solution in PBS for 10 min. After removing the cell culture chamber, the slides were washed with PBS and the cells were embedded in Kaiser's glycerine-gelatin solution. Twelve hours later, confocal microscopy was performed with a Leitz microscope (Leitz DM IRB, Wetzlar, Germany) and a TCS True Confocal Scanner (TCS 4D, Leica, Heidelberg, Germany) equipped with a krypton-argon laser. All optical sections were recorded with the same laser and detector settings and images were processed with the Scanware TCS version 5.1 and Imaris software (Bitplane AG, Zurich, Switzerland).

3. Results and discussion

3.1. Preparation of nanoparticles

The preparation of the methacrylate copolymer nanoparticles was performed by a free radical polymerization process in the presence of ammonium persulfate (APS) as an initiating reagent. The polymerization process followed the methods described in detail in Part I of the present investigation [5]. The monomers used in this study are presented in Fig. 1. In all cases, milky white homogenous particle suspensions were obtained with a yield above 95% of polymerized material as determined by gravimetric measurements. The nanoparticle suspensions were purified by dialysis in order to remove residual monomers, initiator molecules, short chain water soluble polymers and the hydrochloric acid which originated from the polymerization of the employed monomer hydrochlorides. AHMC nanoparticles were also purified by dialysis to remove the trifluoroacetylammonium salt of the *N*-protecting aminohexyl group.

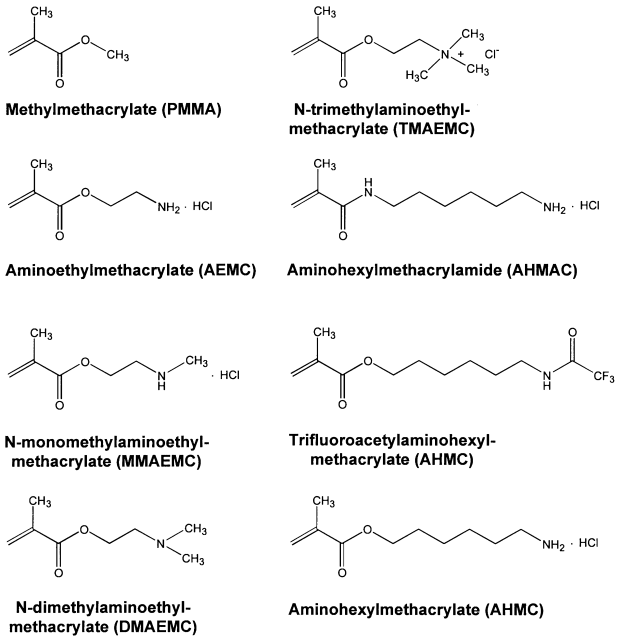

Fig. 1. Chemical structure of the monomers used for the preparation of the aminoalkylmethacrylat copolymer nanoparticles

3.2. Cytotoxicity studies

The potential in vivo toxicity of aminoalkylmethacrylate nanoparticles was estimated on the basis of two in vitro cytotoxicity studies. In the present work, the integrity of mitochondrial enzyme activity was assessed by the MTT tetrazolium salt assay. Metabolic active cells have the capacity to transform the MTT tetrazolium salt into the MTT formazane. Confluent African green monkey kidney cells (AGMK, cell line RITA) were chosen as cell culture model because these cells were used in antiviral test assays for antisense oligonucleotides before [7,10]. The measured extinction of the blue dye obtained by the MTT metabolism after lysis in basic SDS solution correlated to the cell viability. As shown in Table 1, *N*-monomethylaminoethylmethacrylate (MMAEMC), DMAEMC, and AHMAC copolymer nanoparticles did not influence the metabolic activity of mitochondries. The obtained results for these copolymer nanoparticles and for methylmethacrylate (PMMA) homopolymer nanoparticles (not shown) were within the control for untreated cells which was set to 100% even at the highest nanoparticle concentration of 1000 μg/ml. In contrast, AEMC and TMAEMC copolymer caused a concentration dependent decrease of cell viability. The mean nanoparticle concentrations that led to a 50%

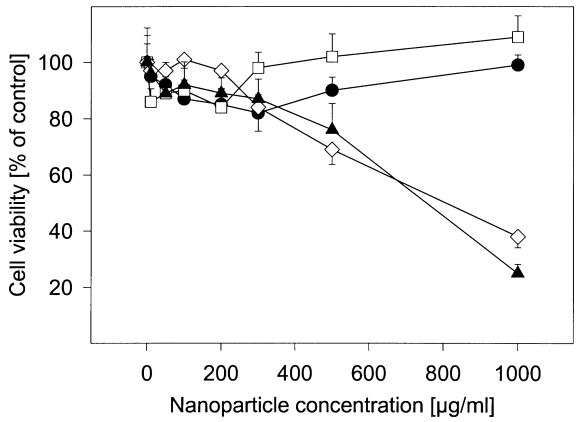

Fig. 2. In vitro cell toxicity of different aminoalkylmethacrylate nanoparticles. AGMK cells were incubated with increasing particle concentrations for 24 h. X: MMAEMC, K: DMAEMC, S: TMAEMC, O: AEMC (mean ± SD, $n = 8$).

reduction of viable cells (IC_{50}) within 4 h incubation were approximately 1000 μg/ml for both, AEMC and TMAEMC copolymer nanoparticles. After 24 h the IC_{50} decreased as cytotoxicity increased (approximately 700 μg/ml for both particle species, Fig. 2). AHMC copolymer nanoparticles were not tested in the present study because they were shown to be cytotoxic to a great extent in preliminary experiments (IC_{50} for 24 h incubation , 100 μg/ml). The cytotoxicity of TMAEMC copolymer nanoparticles was already investigated in a previous study of our group [17]. Unpurified TMAEMC nanoparticle suspensions were shown to reduce cell metabolism in three different cell lines when incubated for 96 h. The IC_{50} for the Vero cells which are derived from the African green monkey kidney cells was found to be about 110 μg/ml after incubation for 96 h. The former result can not be compared directly to the present study because a different cell line was incubated for a longer period of time with unpurified particle suspensions. Additionally, in an earlier study the water soluble DMAEMC homopolymer was shown to influence the metabolism of COS-7 (cells of SV-40-transformed AGMK) cells. One hour incubation with this polymer followed by a subsequent incubation without preparations, led to an IC_{50} of approximately 30 μg/ml [18]. It is very likely that the cationic character of the water soluble polymers was responsible for the observed cytotoxicity. In contrast, we found a higher biocompatibility after copolymerization of DMAEMC with methylmethacrylate which led to the formation of solid nanoparticles with a mixed polymer, offering a slight negative surface charge in PBS at pH 7.4 (zeta

Table 1
In vitro cytotoxic effects of different nanoparticles at a concentration of 1000 μg/ml on African green monkey kidney (AGMK) cells*

	PMMA	AEMC	MMAEMC	DMAEMC	TMAEMC	AHMAC
Incubation (4 h)	107.1 ± 4.4	43.1 ± 6.8	118.3 ± 5.9	85.4 ± 6.7	53.1 ± 6.3	123.0 ± 13.9
Incubation (24 h)	113.1 ± 11.0	25.5 ± 3.3	99.5 ± 3.7	109.3 ± 7.6	38.0 ± 3.9	117.8 ± 8.5

*Results for the cell viability in percent of the untreated cell control (mean ± SD, $n = 8$).

Table 2
Zeta potential (ZP) and nanoparticle diameter (D) of various nanoparticle derivatives measured in solutions of different pH and ionic strength*

Particle derivative	Deionized water		pH 5.5, 10 mM		pH 5.5, 150 mM		PBS pH 7.4, 150 mM	
	ZP (mV)	D (nm)	ZP (mV)	D (nm)	ZP (mV)	D (nm)	ZP (mV)	D (nm)
PMMA	−48.4	183.6	−49.5	176.1	−36.1	196.6	−21.1	186.8
AEMC	+40.4	207.7	+42.5	185.2	+31.8	204.3	+19.0	194.8
MMAEMC	+45.7	254.4	+45.9	238.4	+39.9	253.7	+22.7	251.4
DMAEMC	−8.1	763.8	+8.4	1993.5	+6.8	2183.1	−14.5	107.6
TMAEMC	+64.1	219.4	+37.2	203.5	+28.8	197.4	+26.4	186.0
AHMAC	+44.6	231.3	+42.6	208.1	+33.1	230.3	+20.4	226.3

*Results are mean values of two (D) and six (ZP) independent measurements. PMMA: Polymethylmethacrylate homopolymer nanoparticles. AEMC, MMAEMC, DMAEMC, TMAEMC, and AHMAC: copolymer particles composed of 70% (w/w) Polymethylmethacrylate and 30% (w/w) of the basic copolymer.

potential −14.5 mV, Table 2). Consequently, this copolymerization with the untoxic monomer methylmethacrylate is probably the reason for the reduced toxicity of DMAEMC particles in our study compared with earlier investigations.

The effect of the nanoparticle preparations on the integrity of erythrocyte membranes was investigated in the second in vitro assay of the present cytotoxicity study. Erythrocytes are among the first cells that come into contact with parenterally administered preparations. Therefore, a hemolysis assay will give additional information about the biocompatibility in the case of an in vivo application. Again, as mentioned before, AHMC nanoparticles possessed the highest cytotoxicity. After the incubation at 37°C for 30 min hemolysis was nearly complete, even at a 10-fold lower polymer concentration of 10 mg/ml (data not shown). AEMC nanoparticles were the most toxic particles among the different substituted aminoethyl derivatives (Fig. 3). They caused a 50% hemolysis at a concentration of 100 mg/ml. However, AEMC monomer in the same concentration showed no cytotoxicity at all (hemolysis 2.6%, data not shown).

Therefore, we conclude that the polymerized preparations and not the monomers employed, were responsible for the membrane disrupting effects. MMAEMC copolymer nanoparticles were slightly cytotoxic (15% hemolysis). All other derivatives investigated including the TMAEMC nanoparticles which exhibited a cytotoxic potential in the MTT assay, caused no disruption of the erythrocyte membranes. Presumably hemolysis by TMAEMC nanoparticles would have occurred at higher polymer concentrations. This could not be elucidated because increasing concentrations of the cationic particles led to an aggregation with the negative surfaces of the limited number of erythrocytes present in the test system and, subsequently, aggregation prevented the cell membranes from disruption. Alternatively, binding of released haemoglobin to a surplus of nanoparticles could lead to false negative hemolysis results. As a consequence, it can be concluded that the relative hemolysis decreased with increasing polymer concentration (Fig. 4). As mentioned before, AHMC nanoparticles prepared by polymerization of the *N*-protected derivative trifluoroacetylaminohexylmethacrylate followed by a subsequent amino deprotection under basic conditions were found to be highly cyto-

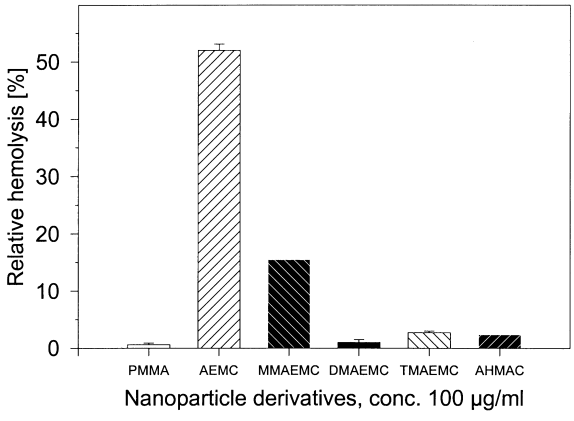

Fig. 3. Hemolytic effects of different aminoalkylmethacrylate copolymer nanoparticles on human erythrocytes in phosphate buffered saline (PBS pH 7.4) at a concentration of 100 mg/ml. Bars represent the mean ± SD (n = 3).

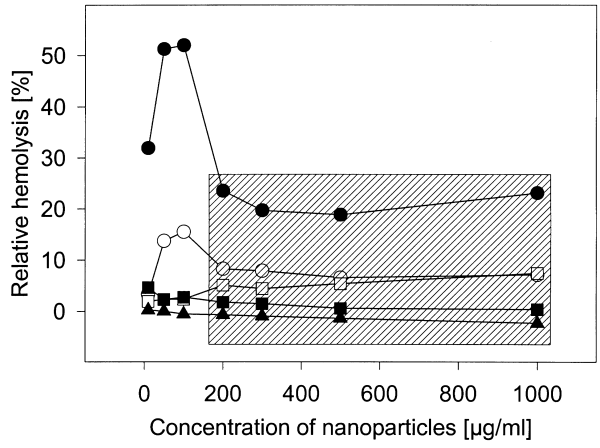

Fig. 4. Dependence of hemolytic effects of different aminoalkylmethacrylate copolymer nanoparticles on human erythrocytes in phosphate buffered saline (PBS pH 7.4) on the particle concentration (mean ± SD, n = 3). X: AEMC, O: MMAEMC, W: AHMAC, B: TMAEMC, O: DMAEMC, lined area: occurrence of aggregation between nanoparticles and oligonucleotides or haemoglobin adsorption, respectively.

toxic. For AHMC nanoparticles exhibiting protected surface aminohexyl groups, no hemolytic effect on erythrocytes was observed (data not shown). In another experiment, AHMC nanoparticles were prepared by a different procedure. The monomer *N*-butyloxycarbonyl-aminohexylmethacrylate was deprotected with hydrochloric acid prior to polymerization. Also by this alternative procedure, the obtained particles caused a complete hemolysis. Surprisingly, aminohexylmethacrylamide showed no cytotoxic potential in both assays, MTT and hemolysis. While the aminohexyl group of the AHMC comonomer was connected to the methacrylate by a C-6 bridge and an ester function, in the case of AHMAC the bonding consisted of a carbamide function. Consequently, the reduced toxicity could be due to the carbamide structure in contrast to the comparable esters, as has been already observed in a previous study [17] for TMAEMC and trimethylaminopropylmethacrylamide (MAPTAC) copolymer nanoparticles. The previous authors proposed an interaction of the positively charged ammonium group with the free electron pair of the amide nitrogen resulting in an intramolecular stabilization. Consequently, the steric hindrance of the interaction between cationic particle surfaces and negatively charged erythrocyte membranes or cell membranes of AGMK cells could be the reason for a reduced toxicity of AHMAC nanoparticles compared to AHMC particles.

Summarizing the results of both assays, the cytotoxicity of aminoalkylmethacrylate copolymer nanoparticles could be attributed to the molecular structure of the employed monomers. The elongation of the monomer alkyl chain by four methylene groups increased the toxicity of the resulting nanoparticles. Furthermore, the integrity of cell membranes was influenced by the substitution of the amino group. The toxic effect of aminoethylmethacrylate nanoparticles could be decreased by the substitution of one or two nitrogen protons by additional methyl groups, whereas the polymerization of monomers exhibiting quaternary ammonium groups led to cytotoxic derivatives. In a previous study, the hemolysis mechanism of a methacrylate derivative was investigated [19]. Liposomes from dipalmitoylphosphatidylcholine were employed in this study as a model for the erythrocyte membrane. It was shown by NMR and DSC measurements that the methacrylate derivative was incorporated into the liposome system and that the phosphatidylcholine polar group (O–C–C–N bond) was affected by the addition of this compound. Therefore, we conclude that the cytotoxic effects of the investigated particle derivatives resulted from the incorporation of aminoalkyl chains into the lipid and/or lipoprotein layers of erythrocyte membranes leading to their disruption and the efflux of haemoglobin. This incorporation was the result of the formation of ion-pairs between positively charged amino groups and the phosphatidyl polar group, as well as hydrophobic interactions between the alkyl portions.

It should be mentioned that only the cytotoxicity assays were able to give some information to predict the in vivo toxicity and, therefore, should not be overvalued. As shown for polyhexylcyanoacrylate nanoparticles, for instance, full cell death occurred in vitro at a concentration of 350 μg/ml whereas in vivo 20 mg/kg PHCA nanoparticles were found to cause no damage or other acute toxic effects to the liver, the organ with highest accumulation after i.v. injection [20].

3.3. Oligonucleotide loading

The antisense oligonucleotide used in our study was complementary to the 3′ acceptor splice junction of Herpes Simplex Virus (HSV 1) pre mRNA 4. Smith et al. [7] and Kulka et al. [8] showed, that this sequence caused a specific reduction of HSV 1 growth. Oligonucleotide loading to previously manufactured nanoparticles was achieved by the formation of ion-pairs between the positively charged aminoalkyl groups located on the particle surface and the negatively charged phosphodiester backbone of the oligonucleotide. The extent of oligonucleotide adsorption was dependent on the portion of the basic copolymer as shown in Fig. 5 for aminohexylmethacrylate methylmethacrylate nanoparticles (AHMC). Copolymerization of methylmethacrylate with increasing concentrations of the aminoalkyl monomer raised the number of amino groups at the particle surface which were protonized under the employed loading conditions (10 mM phosphate buffer, pH 5.5). Pure methylmethacrylate homopolymer nanoparticles (PMMA) exhibited a negative surface charge. Hence, the adsorption of the negatively charged oligonucleotide was not possible due to electrostatic repulsion. As the copolymer content was increased, zeta potential changed into positive values. The zeta potentials and the subsequent loading ratios correlated with the portion of the basic copolymer (Fig. 5). A copolymer content of 30% (w/w) caused the formation of aggregates (mean diameter above 1 μm) because the nanoparticle suspension was no longer stabilized by ionic repulsion forces. Consequently, great standard deviations in loading ratios were observed due to the reduction of the available surface area. Particles made of . 40% (w/w) copolymer showed reproducible significantly increased adsorption of

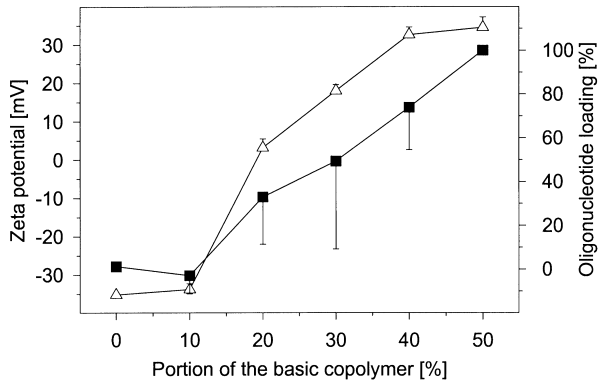

Fig. 5. Influence of the portion of the basic copolymer on zeta potential (K) and oligonucleotide loading (B) of aminohexylmethacrylate methylmethacrylate copolymer nanoparticles (AHMC) (mean ± SD, n = 3–5).

oligonucleotides and led to stable suspensions. At a copolymer content of 50%, the employed oligonucleotide (15 mg/ml) was completely adsorbed onto the particle surfaces (concentration of the nanoparticle suspension 100 mg/ml).

The influence of loading conditions on the adsorption of oligonucleotides was investigated at a constant nanoparticle concentration (100 mg/ml). The preformed particles were incubated at room temperature (20°C) with various oligonucleotide concentrations. The loading conditions were varied by the use of buffers which possessed different pH and ionic strength. Particle characterization indicated that particle size and surface charge of aminoalkylmethacrylate copolymer nanoparticles depended on the pH and on the ionic strength of the medium employed for the loading experiments (Table 2). In media of lower pH values (phosphate buffer solutions, pH 5.5 and deionized water, pH 5.5–6.5) higher surface charges for the basic particles were obtained. At higher salt concentrations, the zeta potential decreased due to competitive adsorption of the phosphate and oligonucleotide anions. Additionally, the hydrodynamic particle diameter determined by PCS decreased, because the reduced surface charge and the lower electrostatic repulsion of the charged amino groups resulted in a more compact polymer configuration. Fig. 6 shows that the amount of oligonucleotide bound to 100 mg methylaminoethyl-methacrylate copolymer nanoparticles (MMAEMC) depended on the medium employed for the loading experiments also.

Phosphate buffer solutions pH 5.5 and deionized water (pH 5.5–6.5) yielded the highest loading. Adsorption decreased drastically when phosphate buffered saline (PBS, pH 7.4, salt concentration 150 mM) was employed. The number of protonized methylaminoethyl groups located at the particle surface was decreased by factor 100 as the pH was increased from 5.5 to 7.4. At this pH, the formation of ion-pairs between the negatively charged oligonucleotide

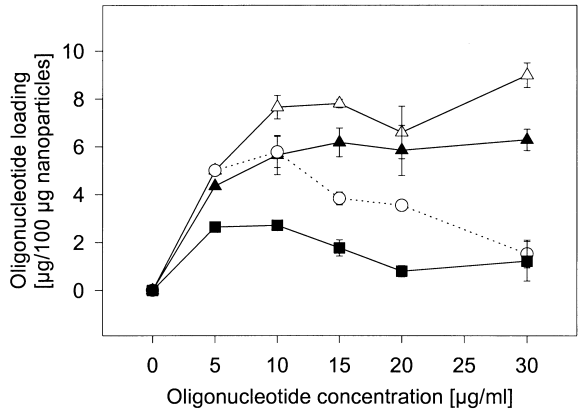

Fig. 6. Influence of the loading medium on oligonucleotide adsorption efficacy. Monomethylaminoethylmethacrylate methylmethacrylate copolymer nanoparticles (MMAEMC) were incubated with oligonucleotide solutions of increasing concentrations at 20°C for 12 h. Loading experiments were performed in (K) 10 mM phosphate buffer, pH 5.5; (K) 150 mM phosphate buffer pH 5.5, (O) deionized water, and (B) phosphate buffered saline pH 7.4, 150 mM (mean ± SD, $n = 3$).

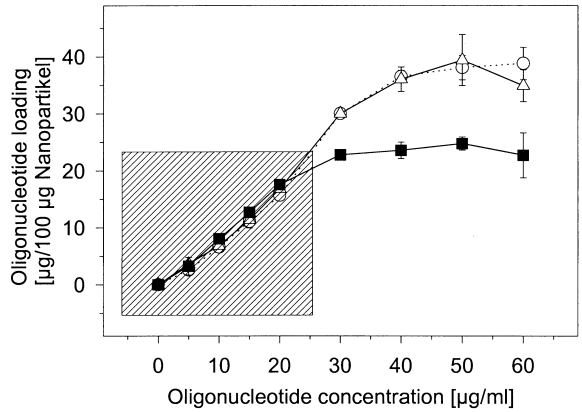

Fig. 7. Influence of the loading medium on oligonucleotide adsorption efficacy. Trimethylaminoethylmethacrylate methylmethacrylate copolymer nanoparticles (TMAEMC) were incubated with oligonucleotide solutions of increasing concentrations at 20°C for 12 h. Loading experiments were performed in (O) deionized water, (K) 10 mM phosphate buffer, pH 5.5, and (B) phosphate buffered saline pH 7.4, 150 mM (mean ± SD, $n = 3$), lined area: linear range of the adsorption profile.

and the positive charged ammonium groups was susceptible to increasing cation concentrations. Hence, the decrease of adsorption was due to the competition of chloric anions and oligonucleotides for free adsorption positions at the particle surfaces.

The decrease in loading at higher oligonucleotide concentrations could be explained by the progress of charge neutralization. A certain oligonucleotide concentration led to an aggregation between nanoparticles and oligonucleotides followed by a subsequent reduction of total surface area which resulted in a lower oligonucleotide binding.

TMAEMC nanoparticles exhibited quarternary ammonium groups which were responsible for a positive charge over the whole pH range. Consequently, the number of positive charged groups remained constant as the pH increased and, as a result, the oligonucleotide adsorption was independent of the loading conditions (lined area in Fig. 7). Particle aggregation was observed at an oligonucleotide concentration above 20 mg/ml in PBS buffer, again leading to lower oligonucleotide loading. Table 3 shows the maximum loading ratios for each particle species. PMMA homopolymer and DMAEMC copolymer nanoparticles were found not to be suitable as carriers for antisense oligonucleotides. DMAEMC representing a tertiary amine exhibited the lowest basicity of the aminoalkyl derivatives and, thus, protonization was hindered. Consequently, only a small amount of oligonucleotides could be adsorbed at pH 5.5. AEMC, MMAEMC, TMAEMC, and AHMC copolymer nanoparticles were suitable carriers for oligonucleotides at each loading condition. It is evident that the substitution of the aminoalkyl group played an important role for the adsorption of the negatively charged drugs. Additional methyl groups connected to the amino group in aminoalkymethacrylate nanoparticles led to a decrease in loading efficacy, probably due to the sterically hindered adsorption. However, TMAEMC copolymer nanoparticles

Table 3

Maximum loading capacities of nanoparticles in media of different pH and ionic strength*

Particle derivative	Loading capacity (mg oligonucleotide/100 mg polymer)		
	Deionized water	pH 5.5, 10 mM	PBS pH 7.4, 150 mM
PMMA	0.24 ± 0.3	0.00 ± 0.59	0.39 ± 0.39
AEMC	17.79 ± 1.55	17.67 ± 1.19	11.05 ± 1.69
MMAEMC	5.77 ± 0.65	8.98 ± 0.51	2.71 ± 0.21
DMAEMC	0.45 ± 0.23	1.66 ± 0.58	0.67 ± 1.36
TMAEMC	38.79 ± 2.84	39.37 ± 4.48	24.74 ± 1.17
AHMC	Not performed	31.30 ± 2.56	Not performed

*Results were derived from adsorption isotherms (mean ± SD, $n = 3$). PMMA: Polymethylmethacrylate homopolymer nanoparticles. AEMC, MMAEMC, DMAEMC, TMAEMC, and AHMAC: copolymer particles composed of 70% (w/w) Polymethylmethacrylate and 30% (w/w) of the basic copolymer.

showed the highest oligonucleotide loading in spite of their maximal steric hindrance due to their quaternary structure. A possible higher charge density compared with the other nanoparticles composed of the same amount of aminoalkylmonomer (30% w/w) could be the reason for this behaviour. During the preparation process, the hydrophilic monomer TMAEMC was enriched at the interface between the growing particles and the aqueous polymerization medium due to its ionic character. Subsequently, a larger number of positively charged substituents were located at the nanoparticle surface.

AHMAC nanoparticles were directly compared with the MMAEMC, DMAEMC and TMAEMC derivatives in another experiment. One hundred micrograms nanoparticles were incubated with 10 mg oligonucleotide using PBS pH 7.4 as dispersion medium. It was shown that the loading efficacy of AHMAC nanoparticles was comparably poor to that of the DMAEMC carriers. The reduced adsorption of oligonucleotides can be contributed to the amide structure of the AHMAC copolymer. Ion-pair formation with the negative oligonucleotide backbone was impeded by the above mentioned interaction of the protonized amino group with the free electron pair of the amide nitrogen.

In a control experiment MMAEMC copolymer nanoparticles were incubated with phosphorothioate modified oligonucleotides as well as 5′-fluorescein labelled oligonucleotides exhibiting the same base sequence as the unmodified phosphodiester oligonucleotides. No significant difference in adsorption efficacy was observed for all oligonucleotide derivatives, because the negatively charged backbone present in all oligonucleotides was responsible for the adsorption to the cationic particle surfaces (data not shown).

3.4. Enzyme protection

The protection against nuclease digestion was determined for the MMAEMC preparation used for the cell-uptake assay. An in vitro enzyme assay using the endonuclease DNase I was applied, as published earlier [10]. Oligonucleotides, 3.94 mg (52.5%) of about 7.50 mg, bound to 100 mg MMAEMC nanoparticles were found to be protected against enzymatic digestion, whereas unbound oligonucleotides resulted a 99.8% enzyme digestion after 30 min. This result demonstrated that a major portion of the adsorbed oligonucleotide was not accessible for the DNase I. However, the oligonucleotide was not completely protected which could also be attributed to the in vitro enzyme assay conditions. Further experiments with oligonucleotide nanoparticle preparations incubated in MEM cell culture medium did not lead to a significant degradation within 4 h. Unprotected oligonucleotides were digested up to 60% in cell culture medium. Corresponding results were also obtained in one of our previous studies with DEAE-dextran nanoparticles [10]. Primarily, the interaction between the positively charged nanoparticle surface and serum proteins was discussed as an additional protective mechanism. Most likely, a coating with serum proteins inhibited the oligonucleotide nanoparticle dissociation as well as the access of nucleases to the nanoparticle surface.

3.5. Cell-uptake

Vero cells were chosen as an in vitro test model for the cell-uptake investigations. This cell line was already employed in a previous study to determine the cell uptake of oligonucleotides [10]. The cells were incubated with either 5′-FITC-labelled oligonucleotides (FODNs) and FODNs adsorbed to MMAEMC nanoparticles at a concentration of 10 mg/ml for 4 h. As mentioned before, this derivative was found to be the most suitable candidate for investigations concerning the toxicological and ODN-loading characteristics. The studies were carried out at two different temperatures (4 and 37°C) to distinguish between active uptake mechanisms and passive diffusion. Cell membranes were stained by the TRITC conjugated plant lectine concanavaline A to localize the cellular distribution of the FODNs. Images of 60 subsequent confocal sections were recorded with a confocal laser scanning microscope (CLSM) and processed using the image processing software. The confocal sections were rearranged to a section image visualizing the horizontal and vertical distribution of fluorescent oligonucleotides and nanoparticles inside the cells. Fig. 8A shows the fluorescence image for FODNs adsorbed to MMAEMC nanoparticles incubated at 37°C. The cells exhibited substantial intracellular fluorescence. This fluorescence was frequently localized in the cytoplasma with a portion present at or close to the plasma membrane. Presumably, cell uptake was not completed after 4 h. Therefore, cells were rinsed with fresh cell culture medium after the removal of the preparations and kept in culture for another 24 h. After the prolonged incubation, no fluorescence was detected at the cell membrane, but was frequently located

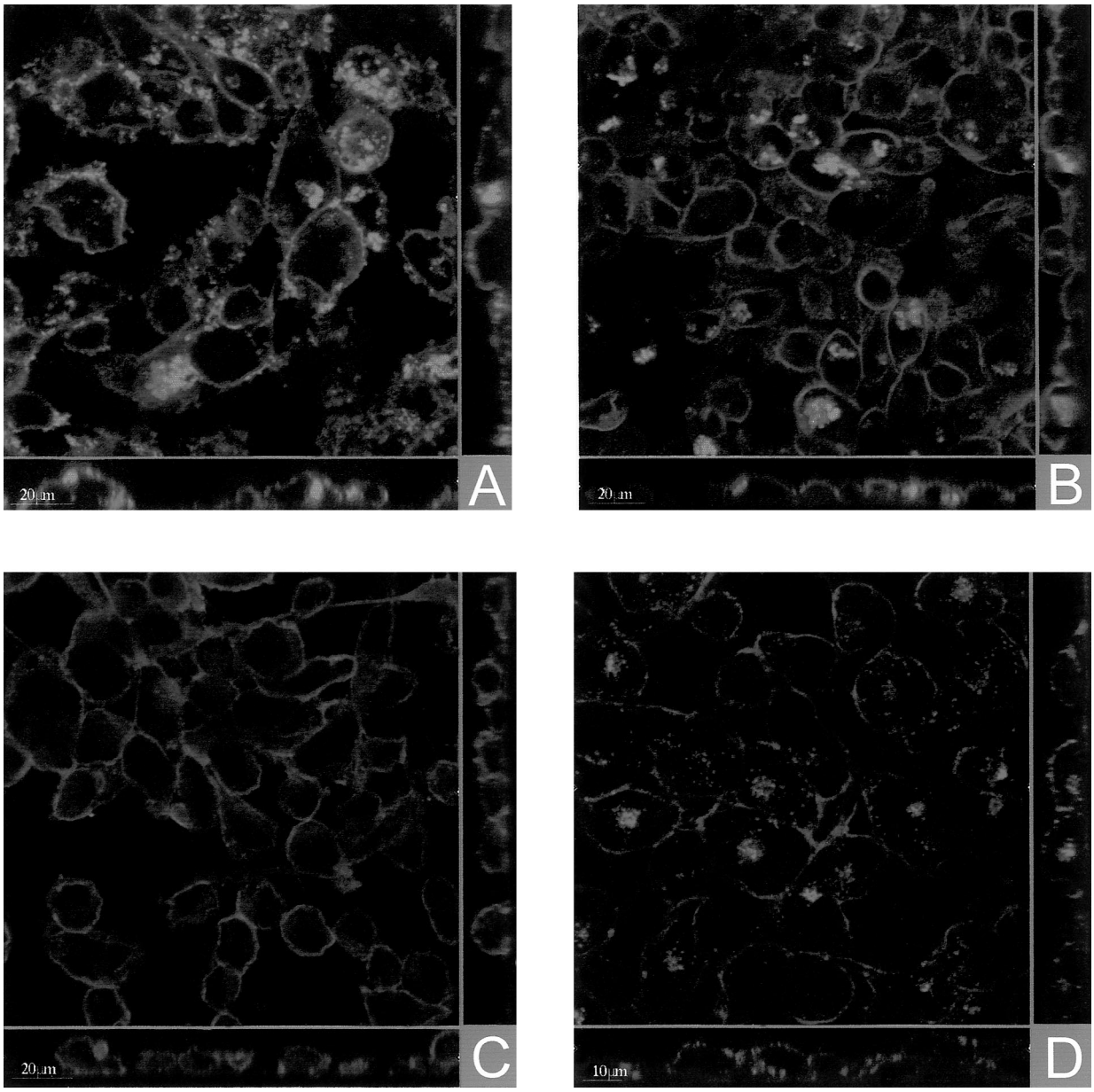

Fig. 8. Penetration of fluorescence-labelled oligonucleotide formulations into Vero cells at 37°C and 5% CO_2. (A) Incubation performed with 10 mg/ml FITC oligonucleotide adsorbed to 100 mg/ml MMAEMC nanoparticles for 4 h. Cell membranes are stained with TRITC-concanavalin A. (B) Incubation performed with 10 mg/ml FITC oligonucleotide adsorbed to 100 mg/ml MMAEMC nanoparticles for 4 h. After the change of medium, cells were kept in culture for further 24 h. (C) Incubation with 10 mg/ml FITC oligonucleotide w/o nanoparticles for 4h. (D) Incubation with 100 mg/ml TRITC-labelled MMAEMC nanoparticles for 4h. Cell membranes are stained with FITC-concanavalin A. All pictures are combined CLSM sections of 60 slices showing horizontal and vertical distribution of the fluorescence.

inside the cells (Fig. 8B). This observation may either be contributed to the internalization of the adsorbed oligonucleotide-nanoparticle complexes or to the degradation of the ODN/NP complexes adsorbed to the cell surfaces. Although in earlier studies some evidence for a receptor mediated endocytotic pathway of unmodified ODNs was reported [21,22], in our study, cellular uptake of unbound oligonucleotides at 37°C was found to be negligible (Fig. 8C). This phenomenon demonstrates that cellular uptake is a paramount problem of an effective pharmaceutical application of unmodified oligonucleotides. These compounds are polyanions, and in general, such substances exhibit a reduced tendency to associate with negatively charged membranes. Additionally, the low cell penetration of free oligonucleotides could be contributed to their instability in culture medium.

No fluorescence at all was observed in cells incubated with unbound FODNs at 4°C. Fluorescence was also mark-

edly decreased when the cells were incubated at 4°C with FODN/NP formulations. The main portion of the FODNs was predominantly localized at the cell surface. Only a small amount of FITC-oligonucleotides was found inside the cells (picture not shown). This observation might be explained by the occurrence of an active transport mechanism such as endocytosis for the internalization of the oligonucleotide/nanoparticle complexes. In a further experiment, the Vero cells were incubated with covalently TRITC-labelled MMAEMC nanoparticles to explore whether these carriers enhanced oligonucleotide uptake only by the adsorption to the cell membranes or if the ODN/NP complexes were totally internalized. As shown in Fig. 8D, again the fluorescence frequently was detectable inside the cells. This experiment was taken as evidence for the uptake of intact MMAEMC nanoparticles into the cells. Comparing this experiment with incubations performed at 4°C, the cellular uptake at 37°C was facilitated by an active and temperature depended transport mechanism.

4. Conclusions

Monomethylaminoethylmethacrylate methylmethacrylate copolymer nanoparticles (MMAEMC) were the most suitable carrier systems for hydrophilic anionic drugs as shown by the cytotoxicity studies and the loading experiments. These cationic particles possessed sufficient adsorption efficacy even at physiological pH under isotonic conditions. Moreover, MMAEMC nanoparticles did not induce cytotoxic effects nor did they significantly influence the integrity of biological membranes. A significant portion of oligonucleotides adsorbed to MMAEMC nanoparticles were protected from enzymatic degradation. In vitro cell-uptake studies also showed that this nanoparticle derivative is an effective uptake enhancer for oligonucleotides.

Acknowledgements

The research was supported by the Deutsche Forschungsgemeinschaft, Bonn, Germany and the Fond der Chemischen Industrie, Frankfurt am Main, Germany. We are grateful to Anja Hildebrand and Christina Spanheimer for their expert technical assistance.

References

[1] J. Kreuter, P.P. Speiser, New adjuvants on a polymethylmethacrylate base, Infect. Immun. 13 (1976) 204–210.
[2] P. Couvreur, M. Roland, P. Speiser, Biodegradable submicroscopic particles containing a biologically active substance and compositions containing them, US Patent 4 (1982) 329–332.
[3] J. Kreuter, Evaluation of nanoparticles as drug-delivery systems. I. Preparation methods, Pharm. Acta Helv. 58 (1983) 196–209.
[4] J. Kreuter, E. Liehl, U. Berg, M. Soliva, P.P. Speiser, Influence of hydrophobicity on the adjuvant effect of particulate polymeric adjuvants, Vaccine 6 (1988) 253–256.
[5] H.-P. Zobel, A. Zimmer, S. Atmaca-Abdel Aziz, M. Gilbert, D. Werner, C.R. Noe, J. Kreuter, F. Stieneker, Evaluation of aminoalkylmethacrylate nanoparticles as colloidal drug carrier systems. Part I: synthesis of monomers, dependence of the physical properties on the polymerization methods, Eur. J. Pharm. Biopharm. 47 (1999) 203–213.
[6] J.L. Tonkinson, C.A. Stein, Antisense nucleic acids – prospects for antiviral intervention, Antivir. Chem. Chemother. 4 (1993) 193–200.
[7] C.C. Smith, L. Aurelian, M.P. Reddy, P.S. Miller, P.O.P. Ts'o, Antiviral effect of an oligo(nucleoside methylphosphonate) complementary to the splice junction of herpes simplex virus type 1 immediate early pre-mRNAs 4 and 5, Proc. Natl. Acad. Sci. USA 83 (1986) 2787–2791.
[8] M. Kulka, C.C. Smith, L. Aurelian, R. Fishelevich, K. Meade, P. Miller, P.O.P. Ts'o, Site specificity of the inhibitory effects of oligo(nucleosidemethylphosphonate)s complementary to the acceptor splice junction of herpes simplex virus type 1 immediate early mRNA 4, Proc. Natl. Acad. Sci. USA 86 (1989) 6868–6872.
[9] L. Necker, L. Whitesell, Antisense technology: biological utility and practical considerations, Am. J. Physiol. 265 (1993) L1–12.
[10] H.-P. Zobel, J. Kreuter, D. Werner, C.R. Noe, G. Kümel, A. Zimmer, Cationic Polyhexylcyanoacrylate nanoparticles as carriers for antisense oligonucleotides, Antisense Nucl. Acid Drug Dev. 7 (1997) 483–493.
[11] C. Chavany, T. Le Doan, P. Couvreur, F. Puisieux, C. Helene, Polyalkylcyanoacrylate nanoparticles as polymeric carriers for antisense oligonucleotides, Pharm. Res. 9 (1992) 441–449.
[12] C. Chavany, T. Saison-Behmoaras, T. Le Doan, F. Puisieux, P. Couvreur, C. Helene, Adsorption of oligonucleotides onto polyisohexylcyanoacrylate nanoparticles protects them against nucleases and increases their cellular uptake, Pharm. Res. 11 (1994) 1370–1378.
[13] G. Godard, A.S. Boutorine, E. Saison-Behmoaras, C. Helene, Antisense effects of cholesterol-oligodeoxynucleotide conjugates associated with poly(alkylcyanoacrylate) nanoparticles, Eur. J. Biochem. 232 (1995) 404–410.
[14] Y. Nakada, E. Fattal, M. Foulquier, P. Couvreur, Pharmacokinetics and biodistribution of oligonucleotide adsorbed onto poly(isobutylcyanoacrylate) nanoparticles after intravenous administration in mice, Pharm. Res. 13 (1996) 38–43.
[15] F. Stieneker, J. Kreuter, Nanoparticles as a potential antigen delivery system, in: J.L. Cleland, R. Langer (Eds.), Formulation and delivery of proteins and peptides. ACS Symposium Series 567, American Chemical Society, Washington, 1994, pp. 306–321.
[16] K. Shiotani, K. Uehata, T. Irie, K. Uekama, D.O. Thompson, V.J. Stella, Differential effects of sulfate and sulfobutyl ether of beta-cyclodextrin on erythrocyte membranes in vitro, Pharm. Res. 12 (1995) 78–84.
[17] F. Hoffmann, J.Cinatl Jr., , H. Kabicova, J. Cinatl, J. Kreuter, F. Stieneker, Preparation, characterization and cytotoxicity of methylmethacrylate copolymer nanoparticles with a permanent positive surface charge, Int. J. Pharm. 157 (1997) 189–198.
[18] J.Y. Cherng, P. van de Wetering, H. Talsma, D.J. Crommelin, W.E. Hennink, Effect of size and serum proteins on transfection efficiency of poly ((2-dimethylamino)ethyl methacrylate)-plasmid nanoparticles, Pharm. Res. 13 (1996) 1038–1042.
[19] S. Fujisawa, Y. Kadoma, Y. Komoda, Hemolysis Mechanism of dental adhesive monomer (methacryloyl-oxydecyl dihydrogen phosphate) Using a phosphatidylcholine liposome system as a model for biomembranes, Dent. Mater. J. 9 (1990) 136–146.
[20] P. Couvreur, L. Grislain, V. Lenaerts, F. Brasseur, P. Guiot, A. Biernacki, Biodegradable polymeric nanoparticles as drug carrier for antitumor agents, in: P. Guiot, P. Couvreur (Eds.), Polymeric Nanoparticles and Microspheres, CRS Press, Boca Raton, 1986, pp. 27–93.

[21] L.A. Yakubov, E.A. Deeva, V.F. Zarytova, E.M. Ivanova, A.S. Ryte, L.V. Yurchenko, V.V. Vlassov, Mechanism of oligonucleotide uptake by cells: involvement of specific receptors? Proc. Natl. Acad. Sci. USA 86 (1989) 6454–6458.

[22] S.L. Loke, C.A. Stein, X.H. Zhang, K. Mori, M. Nakanishi, C. Subasinghe, S. Cohen, L.M. Neckers, Characterization of oligonucleotide transport into living cells, Proc. Natl. Acad. Sci. USA 86 (1989) 3474–3478.